Vector Mesons in Medium and Dileptons in Heavy-Ion Collisions

Ralf Rapp[a] * and Jochen Wambach[b]

[a]Department of Physics and Astronomy, SUNY Stony Brook, New York 11794-3800, USA

[b]Institut für Kernphysik, TU Darmstadt, Schloßgartenstr. 9, D-64289 Darmstadt, Germany

Theoretical approaches to assess modifications of vector mesons in the medium, as well as their experimental identification via electromagnetic probes, are discussed. Implications for the nature of chiral symmetry restoration in hot/dense matter are outlined and put into context with the axialvector channel.

1. Introduction

The investigation of hadron properties inside atomic nuclei constitutes one of the traditional research objectives in nuclear physics. However, in terms of the underlying theory of strong interactions QCD) even the description of the nuclear ground state remains elusive so far. Valuable insights can be expected from a careful study of transition regimes between hadronic and quark-gluon degrees of freedom. *E.g.*, in electron-nucleus scattering experiments the corresponding control variable is the momentum transfer, whereas heavy-ion reactions, performed over a wide range of collision energies, aim at compressing and/or heating normal nuclear matter to witness potential phase transitions into a Quark-Gluon Plasma (QGP).

Among the key properties of the low-energy sector of strong interactions is the (approximate) chiral symmetry of the QCD Lagrangian and its spontaneous breaking in the vacuum. This is evident from such important phenomena as the build-up of a chiral condensate and constituent quark mass ($M_q \simeq 0.4$ GeV), or the large mass splitting of $\Delta M \simeq 0.5$ GeV between 'chiral partners' in the hadron spectrum (such as $\pi(140)$-$\sigma(400-1200)$, $\rho(770)$-$a_1(1260)$ or $N(940)$-$N^*(1535)$). It also indicates that medium modifications of hadron properties can be viewed as precursors of chiral symmetry restoration.

In this talk the focus will be on the vector (V) and axialvector (A) channels. The former is special in that it directly couples to the electromagnetic current (*i.e.*, real and virtual photons) at which point it becomes 'immune' to (strong) final state interactions thus providing direct experimental access to in-medium properties of vector mesons, *e.g.*, through photoabsorption/-production on nuclei, or dilepton (e^+e^-, $\mu^+\mu^-$) spectra in heavy-ion reactions. The key issue is then to relate the medium effects to mechanisms of chiral

*research supported in part by the A.-v.-Humboldt Foundation (Feodor-Lynen program) and U.S. Department of Energy under Grant No. DE-FG02-88ER40388.

restoration. This necessitates the simultaneous consideration of the axialvector channel, which, however, largely has to rely on theoretical analyses.

This talk is structured as follows: Sect. 2 is devoted to vector-meson properties in nuclear matter, Sect. 3 contains applications to heavy-ion reactions and Sect. 4 finishes with conclusions. A more complete discussion of the presented topics can be found in a recent review [1].

2. (Axial-) Vector Mesons in Cold Nuclear Matter

2.1. Correlators and Duality Threshold

The general quantity that is common to most theoretical approaches is the current-current correlation function which in the (axial-) vector channel is defined by

$$\Pi^{\mu\nu}_{V,A}(q) = -i \int d^4x \; e^{iqx} \; \langle 0|\mathcal{T} j^{\mu}_{V,A}(x) j^{\nu}_{V,A}(0)|0\rangle \; . \tag{1}$$

For simplicity we will concentrate on the (prevailing) isospin $I = 1$ (isovector) projections

$$j^{\mu}_{I=1} = \frac{1}{2}(\bar{u} \; \Gamma^{\mu} \; u - \bar{d} \; \Gamma^{\mu} \; d) \quad \text{with} \quad \Gamma^{\mu}_{V} = \gamma^{\mu} \; , \quad \Gamma^{\mu}_{A} = \gamma_5 \gamma^{\mu} \; . \tag{2}$$

At sufficiently high invariant mass both correlators can be described by their (identical) perturbative forms which read (up to α_S corrections)

$$\text{Im} \; \Pi^{\mu\nu}_{V,I=1} = \text{Im} \; \Pi^{\mu\nu}_{A,I=1} = -(g^{\mu\nu} - \frac{q^{\mu}q^{\nu}}{M^2})\frac{M^2}{12} \; \frac{N_c}{2} \; , \quad M \geq M_{dual} \tag{3}$$

($M^2 = q_0^2 - \vec{q}^2$). At low invariant masses the vector correlator is accurately saturated by the (hadronic) ρ spectral function within the Vector Dominance Model (VDM), *i.e.*,

$$\text{Im} \; \Pi^{\mu\nu}_{V,I=1} \;\; = \;\; \frac{(m^{(0)}_{\rho})^4}{g^2_{\rho}} \; \text{Im} \; D^{\mu\nu}_{\rho} \; , \qquad\qquad M \leq M_{dual} \tag{4}$$

$$\text{Im} \; \Pi^{\mu\nu}_{A,I=1} \;\; = \;\; \frac{(m^{(0)}_{a_1})^4}{g^2_{a_1}} \; \text{Im} \; D^{\mu\nu}_{a_1} - f^2_{\pi} \; \pi \; \delta(M^2 - m^2_{\pi}) \; q^{\mu}q^{\nu} \; , \quad M \leq M_{dual} \tag{5}$$

with a similar relation involving the a_1 meson in the axialvector channel. The spontaneous breaking of chiral symmetry (SBCS) manifests itself in both the difference of the a_1 and ρ spectral functions as well as the additional pionic piece in Π_A (notice that f_{π} is another order parameter of SBCS). In vacuum the transition from the hadronic to the partonic regime ('duality threshold') is characterized by the onset of perturbative QCD around $M_{dual} \simeq 1.5$ GeV. In the medium, chiral restoration requires the degeneration of V- and A-correlators over the entire mass range.

2.2. Model-Independent Results: V-A Mixing and Sum Rules

In a dilute gas the prevailing medium effect can be computed via low-density expansions. Using soft pion theorems and current algebra Krippa [2] extended an earlier finite-temperature analysis [3] to the finite-density case to obtain

$$\begin{aligned} \Pi^{\mu\nu}_{V}(q) &= (1-\xi) \; \Pi^{\circ\mu\nu}_{V}(q) + \xi \; \Pi^{\circ\mu\nu}_{A}(q) \\ \Pi^{\mu\nu}_{A}(q) &= (1-\xi) \; \Pi^{\circ\mu\nu}_{A}(q) + \xi \; \Pi^{\circ\mu\nu}_{V}(q) \; ' \end{aligned} \tag{6}$$

i.e., the leading density effect is a mere 'mixing' of the vacuum correlators $\Pi^{\circ\mu\nu}$. The 'mixing' parameter

$$\xi \equiv \frac{4\varrho_N \bar{\sigma}_{\pi N}}{3 f_\pi^2 m_\pi^2} \tag{7}$$

(ϱ_N: nucleon density) is determined by the 'long-range' part of the πN sigma term,

$$\bar{\sigma}_{\pi N} = 4\pi^3 m_\pi^2 \langle N|\pi^2|N\rangle \ \simeq 20 \text{ MeV} \ . \tag{8}$$

Chanfray *et al.* [4] pointed out that $\bar{\sigma}_{\pi N}$ is in fact governed by the well-known nucleon- and delta-hole excitations in the pion cloud of the ρ (or a_1) meson which have been thoroughly studied within hadronic models to be discussed in the following section. A naive extrapolation of eq. (7) to the chiral restoration point where $\xi = 1/2$, gives $\varrho_c \simeq 2.5\varrho_0$, which is not unreasonable. Nonetheless, as we will see below, realistic models exhibit substantial medium modifications beyond the mixing effect.

Similar in spirit, *i.e.*, combining low-density expansions with chiral constraints, is the so-called master formula approach applied in ref. [5]: chiral Ward identities including the effects of explicit breaking are used to express medium corrections to the correlators through empirically inferred πN, ρN (or γN, etc.) scattering amplitudes times density. Resummations to all orders in density cannot be performed either in this framework.

Model independent relations which are in principle valid to all orders in density are provided by sum rules. Although typically of little predictive power, their evaluation in model calculations can give valuable insights. One example are the well-known QCD sum rules which have been used to analyze vector-meson spectral functions in refs. [6,7]. It has been found, *e.g.*, that the generic decrease of the quark- and gluon-condensates on the right-hand-side (*r.h.s.*) is compatible with the phenomenological (left-hand) side if *either* (i) the vector meson masses decrease (together with small resonance widths), *or*, (b) both width and mass increase (as found in most microscopic models).

Another example of sum rules are the ones derived by Weinberg [8], being generalized to the in-medium case in ref. [9]. The first Weinberg sum rule, *e.g.*, connects the pion decay constant to the integrated difference between the V- and A-correlators:

$$f_\pi^2 = -\int_0^\infty \frac{dq_0^2}{\pi(q_0^2 - q^2)} \left[\text{Im } \Pi_V(q_0, q) - \text{Im } \Pi_A(q_0, q)\right] \tag{9}$$

for arbitrary three-momentum q (here, the pionic piece has been explicitly separated out from Π_A). We will come back to this relation below.

2.3. Hadronic Models and Experimental Constraints

Among the most spectacular predictions for the behavior of vector mesons in medium is the Brown-Rho Scaling hypothesis [10]. By imposing QCD scale invariance on a chiral effective Lagrangian at finite density and applying a mean-field approximation it was conjectured that all light hadron masses (with the exception of the symmetry-protected Goldstone bosons) drop with increasing density following an approximately universal scaling law. The scaling also encompasses the pion decay constant (as well as an appropriate power of the quark condensate) and therefore establishes a direct link to chiral symmetry restoration being realized through the vanishing of all light hadron masses.

More conservative approaches reside on many-body techniques to calculate selfenergy contributions to the vector-meson propagators D_V arising from interactions with surrounding matter particles (nucleons). They are computed from gauge-invariant (vector-current conserving) as well as chirally symmetric Lagrangians. The ρ propagator, *e.g.*, takes the form

$$D_\rho^{L,T}(q_0,q;\varrho_N) = \Big[M^2 - (m_\rho^{(0)})^2 - \Sigma_{\rho\pi\pi}^{L,T}(q_0,q;\varrho_N) - \Sigma_{\rho BN}^{L,T}(q_0,q;\varrho_N)\Big]^{-1} \tag{10}$$

for both transverse and longitudinal polarization states (which in matter, where Lorentz-invariance is lost, differ for $q > 0$). $\Sigma_{\rho\pi\pi}$ encodes the medium modifications in the pion cloud (through NN^{-1} and ΔN^{-1} bubbles, so-called 'pisobars') [11–13,6,14], and $\Sigma_{\rho BN}$ stems from direct 'rhosobar' excitations of either S-wave ($N(1520)N^{-1}$, $\Delta(1700)N^{-1}$, ...) or P-wave type (ΔN^{-1}, $N(1720)N^{-1}$, ...) [15–18]. The parameters of the interaction vertices (coupling constants and form factor cutoffs) can be estimated from free decay branching ratios of the involved resonances or more comprehensive scattering data (*e.g.*, $\pi N \to \rho N$ [19], or γN absorption) which determine the low-density properties of the spectral functions. Additional finite-density constraints can be obtained from the analysis of photoabsorption data on nuclei. Invoking the VDM, the total photoabsorption cross section can be readily related to the imaginary part of the in-medium vector-meson selfenergy in the zero mass limit (needed for the coupling to real photons). An example of such a calculation is displayed in Fig. 1 where a reasonable fit to existing data on various nuclei has been achieved. The low-density limit (represented by the long-dashed line in

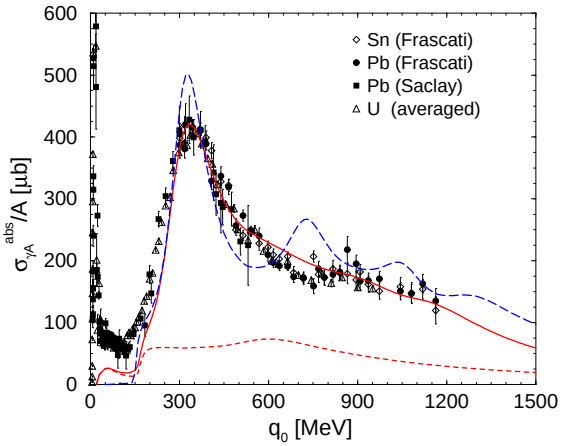

Figure 1. Photoabsorption spectra on nuclei with (full line) and without (long-dashed line) higher order medium effects [18]; short-dashed line: $\Sigma_{\rho\pi\pi}$ contribution.

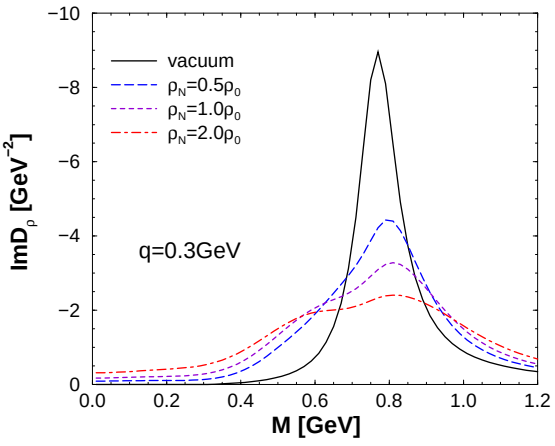

Figure 2. Spin-averaged ρ-meson spectral function in cold nuclear matter [14,20].

Fig. 1) cannot reproduce the disappearance of especially the $N(1520)$ as seen in the data. A selfconsistent calculation to all orders in density [17], however, generates sufficiently large in-medium widths, on the order of $\Gamma_{N(1520)}^{med} \simeq$ 200-300 MeV (resulting in the full line).

Fig. 2 shows the final result for the ρ spectral function [20] which has been subjected to the aforementioned constraints. The apparent strong broadening is consistent with other

calculations [6,17]. Similar features, albeit less pronounced, emerge within analogous treatments for ω and ϕ mesons [6].

Let us now return to the question what these findings might imply for chiral restoration. In a recent work by Kim *et al.* [21] an effective chiral Lagrangian including a_1-meson degrees of freedom has been constructed. Medium modifications of the latter are introduced by an 'a_1-sobar' through $N(1900)N^{-1}$ excitations to represent the chiral partner of the $N(1520)N^{-1}$ state. Pertinent (schematic) two-level models have been employed for both the ρ and a_1 spectral densities which, in turn, have been inserted into the Weinberg sum rule, eq. (9) (supplemented by perturbative high energy continua). The resulting

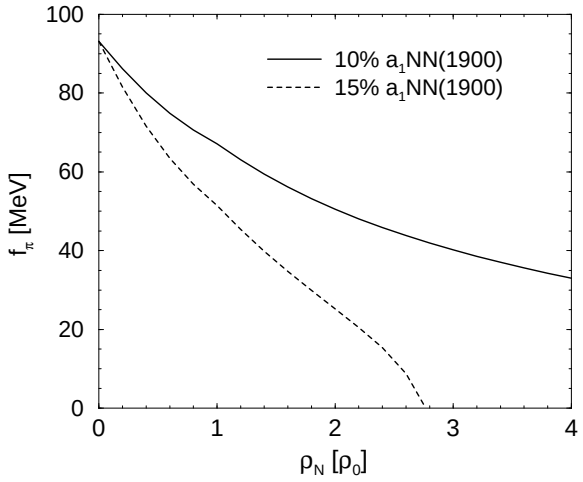

Figure 3. Pion decay constant at finite density when evaluated through the Weinberg sum rule using schematic two-level models for in-medium ρ and a_1 spectral functions [21].

density-dependence of the pion decay constant, displayed in Fig. 3, exhibits an appreciable decrease of $\sim 30\%$ at $\varrho_N = \varrho_0$, which bears some sensitivity on the assumed branching ratio of the $N(1900) \to N a_1$ decay (or $N(1900)N a_1$ coupling constant). However, the mechanism is likely to be robust: due to the low-lying ρ-$N(1520)N^{-1}$ and a_1-$N(1900)N^{-1}$ excitations, accompanied by a broadening of the elementary resonance peaks, the ρ and a_1 spectral densities increasingly overlap, thus reducing f_π.

3. Electromagnetic Observables in Heavy-Ion Reactions

In central collisions of heavy nuclei at (ultra-) relativistic energies (ranging from p_{lab}=1-200 AGeV in current experiments to $\sqrt{s}$=0.2-10 ATeV at RHIC and LHC) hot and dense hadronic matter is created over extended time periods of about 20 fm/c. Local thermal equilibrium is probably reached within the first fm/c, after which the 'fireball' expands and cools until the strong interactions cease ('thermal freezeout') and the particles stream freely to the detector. Electromagnetic radiation (real and virtual photons) is continuously emitted as it decouples from the strongly interacting matter at the point of creation.

The thermal production rate of e^+e^- pairs per unit 4-volume can be expressed through

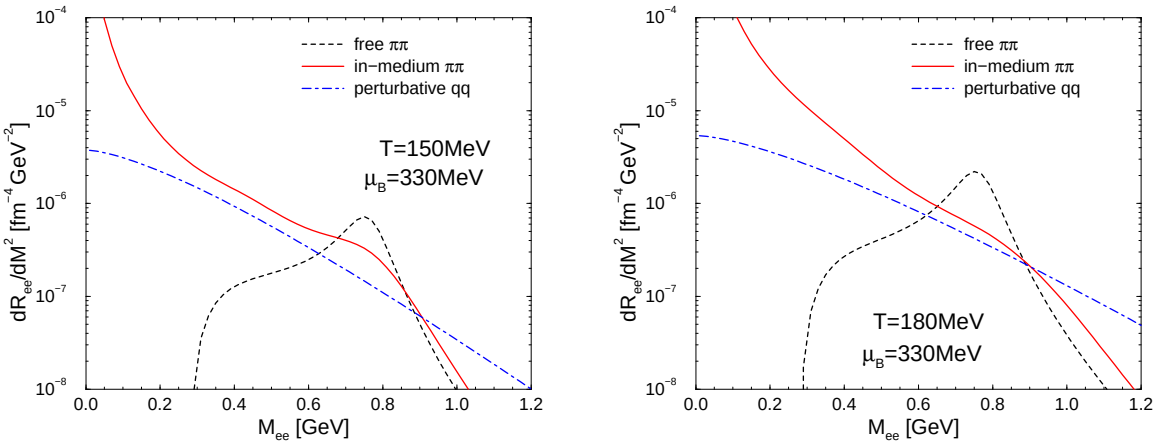

Figure 4. e^+e^- production rates in hot hadronic matter from free $\pi^+\pi^-$ (dashed line), in-medium $\pi^+\pi^-$ (full line) [20] and $\mathcal{O}(\alpha_S^0)$ $q\bar{q}$ annihilation (dashed-dotted line).

the electromagnetic current correlation function (summed over all isospin states I=0,1),

$$\frac{dN_{ee}^{th}}{d^4x d^4q} = -\frac{\alpha^2}{\pi^3 M^2}\, f^B(q_0;T)\, \frac{1}{3}\, (\text{Im}\ \Pi_{em}^L + 2\text{Im}\ \Pi_{em}^T) \tag{11}$$

(f^B: Bose distribution function; a similar expression holds for photons with $M \to 0$). Fig. 4 shows that the medium effects in the ρ propagator (including interactions with nucleons as well as thermal pions, kaons, etc.) induce a substantial reshaping of the emission rate (full lines) as compared to free $\pi\pi$ annihilation (dashed line) already at rather moderate temperatures and densities (left panel). In fact, under conditions close to the expected phase boundary (right panel) the ρ resonance is completely 'melted' and the hadronic dilepton production rate is very reminiscent to the one from a perturbative Quark-Gluon Plasma (dashed-dotted lines in Fig. 4) down to rather low invariant masses of ~ 0.5 GeV (α_S corrections to the partonic rate might improve the agreement at still lower masses). It has been suggested [20] to interpret this as a lowering of the in-medium quark-hadron duality threshold as a consequence of the approach towards chiral restoration.

The total thermal yield in a heavy-ion reaction is obtained by a space-time integration of eq. (11) over the density-temperature profile for a given collision system, modeled, *e.g.*, within transport [22] or hydrodynamic [23] simulations. At CERN-SpS energies (160–200 AGeV) this 'thermal' component is dominant over (or at least competitive with) final state hadron decays (at low M) and hard initial processes such as Drell-Yan annihilation (at high M) in the invariant mass range $M \simeq 0.2$-2 GeV. A consistent description of the measured data [24–27] is possible once hadronic many-body effects are included [20,28,29], cf. Figs.5 and 6. However, at this point also the dropping mass scenario [10] is compatible with the data [30] (cf. dashed curve in Fig. 5).

Optimistically one may conclude that strongly interacting matter close to the hadron-QGP phase boundary has been observed at the CERN-SpS. Other observables such as hadro-chemistry [31] or J/Ψ suppression [32] also support this scenario. Nonetheless, further data are essential to substantiate the present status and resolve the open questions.

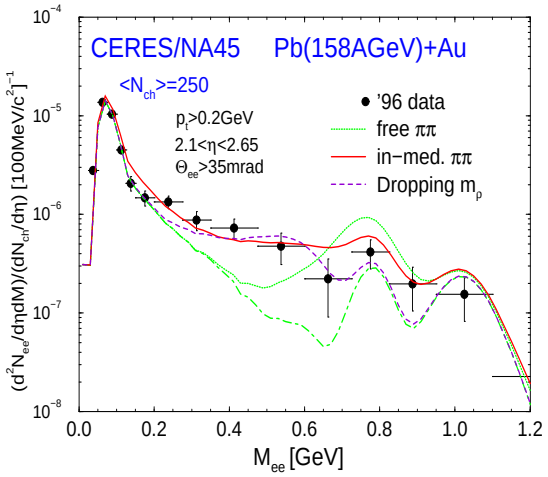

Figure 5. Low-mass dilepton spectra at the CERN-SpS [25]; Dashed-dotted line: particle decays after freezeout (hadronic 'cocktail'), other lines: cocktail + $\pi\pi$ annihilation as indicated.

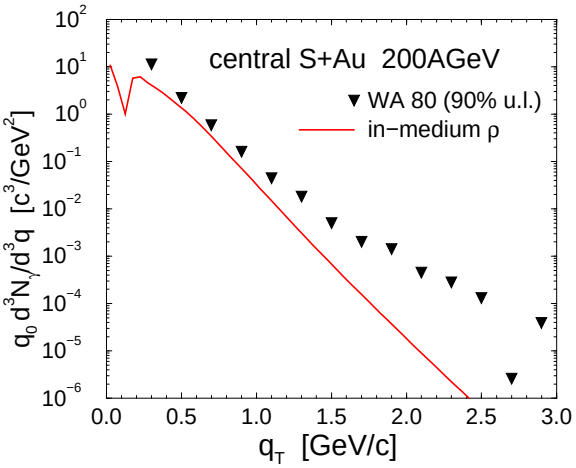

Figure 6. Direct photon spectra at the CERN-SpS: upper limits as extracted from the WA80 experiment [24] compared to in-medium thermal radiation contributions (full line) [1].

4. Conclusions

This talk has focused on medium modifications of vector mesons in connection with chiral symmetry restoration in hot/dense matter. In accordance with a variety of empirical information hadronic spectral functions are characterized by the appearance of low-lying excitations as well as a broadening of the resonance structures. A schematic treatment of the a_1 meson on similar footings shows that these features encode an approach towards chiral restoration in nuclear matter as signaled by the decrease of the pion decay constant when evaluating the first Weinberg sum rule.

The application of these model calculations to electromagnetic observables as measured in recent heavy-ion experiments at the CERN-SpS leads to a reasonable description of the data from 0 to 2 GeV in invariant mass. The structureless in-medium hadronic dilepton production rates resemble perturbative $q\bar{q}$ annihilation in the vicinity of the expected phase boundary indicating that chiral restoration might be realized through a reduction of the quark-hadron duality threshold which in vacuum is located around 1.5 GeV. It would also corroborate the interrelation between temperature/density and momentum transfer in the transition from hadronic to partonic degrees of freedom.

In the near future further dilepton data will be taken by the PHENIX experiment [34] at RHIC (advancing to a new energy frontier) as well as the precision experiment HADES [33] at GSI. Thus electromagnetic observables can be expected to continue the progress in our understanding of strong interaction physics.

Acknowledgments

It is a pleasure to thank G.E. Brown, E.V. Shuryak and H. Sorge for collaboration and many fruitful discussions.

REFERENCES

1. R. Rapp and J. Wambach, to appear in Adv. Nucl. Phys. (2000), and hep-ph/9909229.
2. B. Krippa, Phys. Lett. **B427** (1998) 13.
3. M. Dey, V.L. Eletsky and B. Ioffe, Phys. Lett. **B252** (1990) 620.
4. G. Chanfray, J. Delorme, M. Ericson and M. Rosa-Clot, nucl-th/9809007.
5. J.V. Steele, H. Yamagishi and I. Zahed, Phys. Rev. **D56** (1997) 5605.
6. F. Klingl, N. Kaiser and W. Weise, Nucl. Phys. **A624** (1997) 527.
7. S. Leupold, W. Peters and U. Mosel, Nucl. Phys. **A628** (1998) 311.
8. S. Weinberg, Phys. Rev. Lett. **18** (1967) 507.
9. J.I. Kapusta and E.V. Shuryak, Phys. Rev. **D49** (1994) 4694.
10. G.E. Brown and M. Rho, Phys. Rev. Lett. **66** (1991) 2720.
11. M. Herrmann, B. Friman and W. Nörenberg, Nucl. Phys. **A560** (1993) 411.
12. G. Chanfray and P. Schuck, Nucl. Phys. **A555** (1993) 329.
13. M. Asakawa, C.M. Ko, P. Lévai and X.J. Qiu, Phys. Rev. **C46** (1992) R1159.
14. M. Urban, M. Buballa, R. Rapp and J. Wambach, Nucl. Phys. **A641** (1998) 433.
15. B. Friman and H.J. Pirner, Nucl. Phys. **A617** (1997) 496.
16. R. Rapp, G. Chanfray and J. Wambach, Nucl. Phys. **A617** (1997) 472.
17. W. Peters *et al.*, Nucl. Phys. **A632** (1998) 109.
18. R. Rapp, M. Urban, M. Buballa and J. Wambach, Phys. Lett. **B417** (1998) 1.
19. B. Friman, in Proc. of ACTP Workshop on 'Hadron Properties in Medium' (Seoul, Korea, 27.-31.10.97); and nucl-th/9801053.
20. R. Rapp and J. Wambach, Eur. Phys. J. **A** in press, and hep-ph/9907502; R. Rapp, Proc. of Quark Matter '99 (Torino, Italy, 10.-15.05.99), to appear in Nucl. Phys. **A**, and hep-ph/9907342.
21. Y. Kim, R. Rapp, G.E. Brown and M. Rho, nucl-th/9912061.
22. W. Cassing and E.L. Bratkovskaya, Phys. Rep. **308** (1999) 65.
23. J. Sollfrank *et al.*, Phys. Rev. **C55** (1997) 392; C.M. Hung and E.V. Shuryak, Phys. Rev. **C56** (1997) 453.
24. R. Albrecht *et al.*, WA80 collaboration, Phys. Rev. Lett. **76** (1996) 3506.
25. G. Agakichiev *et al.*, CERES collaboration, Phys. Lett. **B422** (1998) 405; B. Lenkeit, Doctoral Thesis, University of Heidelberg, 1998.
26. A.L.S. Angelis *et al.* (HELIOS-3 collaboration), Eur. Phys. J. **C5** (1998) 63.
27. E. Scomparin *et al.* (NA50 collaboration), J. Phys. **G25** (1999) 235; P. Bordalo *et al.* (NA50 collaboration), Proc. of Quark Matter '99 (Torino, Italy, 10.-15.05.99), to appear in Nucl. Phys. **A**.
28. R. Rapp and E.V. Shuryak, Phys. Lett. **B** in press, and hep-ph/9909348.
29. K. Gallmeister, B. Kämpfer and O.P. Pavlenko, hep-ph/9909379.
30. G.Q. Li, C.M. Ko, G.E. Brown and H. Sorge, Nucl. Phys. **A611** (1996) 539; G.Q. Li and C. Gale, Phys. Rev. **C58** (1998) 2914.
31. P. Braun-Munzinger and J. Stachel, Nucl. Phys. **A638** (1998) 3c.
32. H. Satz, Proc. of Quark Matter '99 (Torino, Italy, 10.-15.05.99), to appear in Nucl. Phys. **A**, and hep-ph/9908339.
33. J. Friese, these proceedings.
34. see, *e.g.*, the PHENIX homepage at http://www.phenix.bnl.gov.